Compact Stellarator Coils

N. Pomphrey[1], L. Berry[2], A. Boozer[3], A. Brooks[1], R. Hatcher[1], S. Hirshman[2], L-P. Ku[1], W. Miner[4], H. Mynick[1], W. Reiersen[1], D. Strickler[2], P. Valanju[4]

[1] Princeton Plasma Physics Laboratory, Princeton, NJ 08543, USA
[2] Oak Ridge National Laboratory, Oak Ridge, TN 37831-8070, USA
[3] Dept of Applied Physics, Columbia University, New York, NY 10027, USA
[4] University of Texas at Austin, Austin, TX 78712-1081, USA

e-mail contact of main author: pomphrey@pppl.gov

Abstract

Experimental devices to study the physics of high-beta ($\beta \gtrsim 4\%$), low aspect ratio ($A \lesssim 4.5$) stellarator plasmas require coils that will produce plasmas satisfying a set of physics goals, provide experimental flexibility, and be practical to construct. In the course of designing a flexible coil set for the National Compact Stellarator Experiment, we have made several innovations that may be useful in future stellarator design efforts. These include: the use of Singular Value Decomposition methods for obtaining families of smooth current potentials on distant coil winding surfaces from which low current density solutions may be identified; the use of a Control Matrix Method for identifying which few of the many detailed elements of a stellarator boundary must be targeted if a coil set is to provide fields to control the essential physics of the plasma; the use of a Genetic Algorithm for choosing an optimal set of discrete coils from a continuum of potential contours; the evaluation of alternate coil topologies for balancing the tradeoff between physics objective and engineering constraints; the development of a new coil optimization code for designing modular coils, and the identification of a "natural" basis for describing current sheet distributions.

1 Introduction

Experimental devices to study the physics of high-beta ($\beta \gtrsim 4\%$), low-aspect-ratio ($A \lesssim 4.5$) stellarator plasmas require coils that will produce plasmas satisfying a set of physics goals, provide experimental flexibility, and be practical to construct.

In the first stage of stellarator design, baseline plasma configurations with attractive equilibrium physics properties are identified using a fixed-boundary configuration optimization procedure originally developed by Nuhrenberg and Zille[1]. Here the plasma boundary shape is varied, with assumed current and pressure profiles and toroidal flux in the plasma, so as to best satisfy chosen stability and transport goals. There remains the complicated task of designing a flexible coil set which can provide magnetic fields which support the reference equilibria and which allow a wide range of interesting physics experiments around the design configuration. In the course of designing a coil set for the National Compact Stellarator Experiment (NCSX), we have made several innovations that we expect to be useful in future stellarator design efforts. Although NCSX is a quasi-axisymmetric (QA) device the methods described here should be applicable to any low-aspect-ratio stellarator design.

2 Current Sheet Coil Improvements using SVD

The NESCOIL code[2] has been an important coil design tool for larger aspect ratio stellarators, and continues to be used in the design of NCSX. A coil winding surface (CWS) is chosen that encloses the plasma and has realistic coil-to-plasma separations. A current potential $\Phi(u,v)$ representing a surface current distribution $\vec{j}' = \hat{n}' \times \nabla\Phi(u,v)$ is then sought such that the normal component of the magnetic field vanishes in the least-squares sense at the plasma boundary ($\hat{n}$ and $\hat{n}'$ are unit normals to the plasma and coil winding surface, and u, v are poloidal and toroidal angles per field period on the CWS). Once the potential is determined, discrete coils are obtained by selecting an appropriate set of contours of Φ and interpreting each contour as a filamentary coil carrying an amount of current that is proportional to the change in potential midway between the chosen contour and its two chosen neighbours. Problems can be encountered with this standard NESCOIL procedure when it is applied to a CWS distant from the plasma: Numerical difficulties are associated with ill-conditioning of the inductance equations which relate the Fourier components of the current potential to the normal component of the magnetic field at the plasma boundary, and these can result in excessively large current densities in the current sheet solution. To overcome this problem and to obtain smooth current potential solutions we have implemented a Singular Value Decomposition (SVD)[3] method for solving the inductance equations. By varying the number of singular values retained in the SVD solution, a family of current sheet solutions is obtained which represents a tradeoff between the fitting error (related to the accuracy of reconstructing the target plasma from the coils) and engineering criteria such as coil complexity and current density[4].

In general, the current potential on a prescribed CWS enclosing a chosen plasma can be written as the sum of a secular and a periodic contribution[2]:

$$\Phi(u,v) = c_t u + c_p v + \sum_{m=0,M,n=-N,N} \Phi_{mn} \sin 2\pi(mu + nv). \qquad (1)$$

Non-zero secular coefficients c_t and c_p correspond to coil topologies with net poloidal and toroidal currents (e.g., stellarator modular coils or axisymmetric poloidal field coils).

A saddle coil design with $c_t = c_p = 0$ is being considered for NCSX. In this option the toroidal flux requirements of the plasma would be provided by tokamak field coils providing a $1/R$ toroidal field. The saddle coils would provide the required stellarator transform.

Figure 1 shows results from the calculation of a family of current sheet solutions with saddle topology for a candidate NCSX plasma named LI383 ($< R >= 1.73m, < a >= 0.40m, \beta = 4\%, I_p = 150kA, B_T = 1.2T$). A CWS with a coil-to-plasma normal separation distance varying between 18 cm and 25 cm was used. The inductance equations, $\mathbf{LI} = \mathbf{b}$, relating the Fourier coefficients $\mathbf{I} = \{\Phi_{mn}\}$ of the current potential to the normal component of the magnetic field $\mathbf{b} = \{(\vec{B} \cdot \hat{n})(u,v)_i\}$ on the plasma boundary were solved using SVD. The $\mathbf{b}$ data were evaluated on a 64 x 64 mesh of points on the plasma boundary, uniformly spaced in u, v. Maximum poloidal and toroidal modenumbers used in the Fourier representation of Φ were $M = 8, N = 8$ which lead to row and column dimensions for $\mathbf{L}$ of $N_b = 4096$ and $N_\Phi = 144$, respectively. $N_\Phi = 144$ approximate solutions of the inductance equation were obtained using the following procedure: For $j = 1, ..., N_\Phi$, all but the largest j singular values are set to zero for the calculation of the pseudoinverse[3] of $\mathbf{L}$. Once the pseudoinverse is calculated, the solution vector $\mathbf{I}$ for the given value of j is determined by standard back-substitution. For $j = N_\Phi$, the solution is identical to the standard NESCOIL least-squares solution. For $j < N_\Phi$ the solutions are further regularized by the SVD cutoff, allowing a trade-off between accuracy of solution and maximum current density of the current sheet. The accuracy of solution is characterized by B_{err}^{rms} and B_{err}^{max}, the r.m.s. and maximum normal components of the magnetic field error on the plasma boundary normalized by the local total magnetic field. B_{err}^{rms} in particular is a measure of how well the current sheet solution can reconstruct the shape of the target equilibrium, and in practice we find that $B_{err}^{rms} \lesssim 1\%$ is required for accurate reconstruction of QA configurations. From Fig. 1 we see an essentially monotonic dependence of the fitting errors on the number of singular values retained. However, the dependence of the calculated sheet current density, J^{max}, on j is non-monotonic. By selecting the particular current sheet obtained by retaining 126 finite singular values, and using this sheet for cutting coils (see Sec. 4), the current sheet density is reduced by 10% compared with the standard least-squares NESCOIL solution. In other cases, reductions of up to 50% have been achieved. Such reductions lead to a significant increase in allowed flattop time for the coils.

3 Control Matrix Method for Sensitivity Analysis

The ability to control kink stability and quasi-axisymmetry are key elements of the proposed NCSX experiment. As reported previously for an early candidate QA configuration named c82[5] (with similar physics properties to LI383) it was found that increasing/decreasing the outboard indentation of the plasma cross section at the symmetry plane $v = 0.5$, relative to the baseline indentation, stabilizes/destabilizes external kink modes. Further, specific coil groups were identified which could perform this kink mode control. However, as the kink growth rate was varied substantial departures from quasi-axisymmetry developed. To determine which combination of coil currents can independently control the kink stability and QA, it is helpful to understand the specific plasma shape changes which affect these physics properties. Control matrices[6] provide this information.

Consider a plasma configuration, $\mathbf{Z}$ which is associated with a set of M targeted physics

properties, $\mathbf{P}$. For example, $\mathbf{Z}$ can be taken to be the set of N Fourier components which describe independent displacements of the plasma boundary. The physics parameters can be such quantities as iota, and various measures of QA transport and stability such as $\chi_T^2 = \sum_{m,n\neq 0} B_{mn}^2/B_{00}^2$ on one or more chosen flux surfaces in the plasma, and $\chi_K^2 = \lambda_{Kink}^2$. Expanding $\mathbf{P}(\mathbf{Z} = \mathbf{Z_0} + \mathbf{z}) = \mathbf{P}(\mathbf{Z_0}) + \mathbf{p}$ about a particular configuration $\mathbf{Z_0}$ one has to first order a matrix equation

$$\mathbf{p} = \mathbf{C_0} \cdot \mathbf{z}, \tag{2}$$

with $\mathbf{C_0} \equiv \mathbf{C}(\mathbf{Z_0})$ the control matrix at design point $\mathbf{Z_0}$. This may be inverted using the SVD theorem[3] $\mathbf{C_0} = \mathbf{U} \cdot \mathbf{\Sigma} \cdot \mathbf{V^T}$ with $\mathbf{U}, \mathbf{V}$ unitary matrices and Σ a diagonal matrix of singular values σ_i. Taking the particular basis set $\pi^{i=1,M}$ in the target $\mathbf{P}$-space to be the set of unit vectors with 1 in the i^{th} position and 0 elsewhere, one has the corresponding set of $\xi^{\mathbf{i}}$ displacements in $\mathbf{Z}$-space

$$\xi^{\mathbf{i}} \equiv \mathbf{C_0^+} \cdot \pi^{\mathbf{i}}, \tag{3}$$

with $\mathbf{C_0^+}$ the pseudoinverse of C_0. The $\xi^{\mathbf{i}}$ physically represent displacements which change a single physics parameter, such as the kink mode growth rate ($i = K$) or QA transport ($i = T$) leaving the other parameters unchanged. The $(N - M)$ vectors $\mathbf{v^i}(i = M + 1, \ldots, N)$ spanning the nullspace of $\mathbf{C}$ (which change the configuration without modifying any of the P_i) are the orthonormal set formed by those columns of $\mathbf{V}$ with i such that $\sigma_i = 0$. These are also important, permitting one to find different stellarator boundaries with the same physics performance, but different engineering properties, giving flexibility for improved coil design. Figure 2 shows results from a calculation of the displacement vectors $\xi^{\mathbf{T,K}}$ for a member of the c82 family of configurations. A notable success of the CM calculation is the manifestation of $\xi^{\mathbf{K}}$ as outboard indentation at the $v = 0.5$ plane, as observed empirically. If stellarator coils can exactly reproduce this boundary displacement, there will be no modification of the QA-ness.

4 A Genetic Algorithm for Cutting Discrete Coils

Once the current potential $\Phi(u, v)$ is calculated from NESCOIL, a set of discrete coils can be obtained by selecting N_c appropriate contours of Φ and interpreting each as a filamentary coil. In the limit as $N_c \to \infty$ the discrete coil system reproduces exactly the magnetic field of the current sheet. For a practical coil system, however, we must choose a coil set with the following minimum set of properties: (1) the number of coils should be small, to allow for heating and diagnostics; (2) the reconstruction errors (measured by how well the boundary conditions $\mathbf{b} = \mathbf{0}$ are satisfied at the plasma boundary) should satisfy $B_{err}^{rms} \lesssim 1\%$, and (3) the maximum coil current should be small ($< 20kA/cm^2$) to minimize resistive dissipation which limits the flat-top time of the magnetic field. Various algorithms have been explored for choosing the optimum set of contours to consider as coils. Among these, a Genetic Algorithm(GA)[7], which is an adaptive search and optimization method that simulates natural evolution processes of biological organisms, has been found to greatly improve our ability to find coil designs which realize the coil design targets (maximum current density, coil complexity, etc).

GA's work with a population of 'individuals' each of which represents a possible solution to the optimization problem. An individual is assigned a 'fitness' according to how well it satisfies the optimization targets. In the present application, an individual

is defined to be a particular subset of potential contours, and the fitness measure is a linear combination of B_{err}^{rms} and I_c^{max}. The fittest individuals are allowed to reproduce by cross-breeding, thereby producing a new generation of individuals (population of new solutions) that contains a high proportion of the best characteristics of the previous generation. In this way, over successive generations, good characteristics are spread throughout the population and the most promising areas of the search space are explored. The GA incorporates "mutation" during evolution, which encourages finding the global, rather than a local, minimum state.

Full details of the GA applied to the problem of cutting stellarator coils are presented in ref. [8]. Here, we simply demonstrate the usefulness of this coil-cutting algorithm in obtaining discrete saddle coils for the c82 plasma configuration, by comparing results using the GA with those from the conventional algorithm which chooses N_c contours equally spaced in Φ, having equal currents in each of the coils. To achieve $B_{err}^{rms} \leq 1\%$ with equally spaced contours, it was found necessary to have $N_c = 13$ coils per half-period. This gives a corresponding maximum coil current density of $I_c^{max} = 14.7 kA/cm^2$. Table 1 shows results from a sequence of GA runs assuming different values of N_c and targeting a linear combination of B_{err}^{rms} and I_c^{max} in the cost (fitness) function. The GA is seen to reduce the number of required coils by a factor of 3 while achieving equal, or somewhat lower, values for the targeted quantities. The coil contours selected by the GA are shown as thick lines in Fig. 3.

5 Alternate Coil Topologies

Plasma configurations and conformal saddle coil designs for NCSX were initially generated based on maximizing the use of existing assets from the PBX tokamak. In particular, the required toroidal flux was supplied from the $1/R$ field of the tokamak toroidal field (TF) coils. For the c82 plasma configuration, this resulted in high current densities in even highly optimized saddle coil designs (e.g., see Table 1). Alternate coil topologies have been explored around the c82 plasma configuration in parallel with the development of alternate plasma configurations. The goal is to identify the key characteristics of each topology, including plasma properties (performance, flexibility, and surface quality), machine constructability, access, performance (toroidal field and pulse length), and cost, with a view to decreasing engineering difficulties. Coil topologies considered include saddle coils with $1/R$ background TF coils, saddle coils with L=3 background coils, and modular coils. For comparing the options on an equal footing, a simple coil selection strategy was used: Saddle and modular coils were obtained from equi-potential contours of the current sheet potential, retaining the minimum number of filamentary coils needed to reduce the B-normal fitting error at the plasma boundary to $B_{err}^{rms} = 1\%$. As demonstrated in Sec. 4, such a strategy results in the need for a larger number of saddle coils than the GA.

The $1/R$ background field option features vertical TF coils and circular poloidal field (PF) coils for equilibrium flexibility and inductive current drive and is shown in Fig. 4. Saddle coils are located in a monolithic shell (the CWS) that surrounds the plasma surface. This option maximizes the use of existing assets from the PBX tokamak, which should translate into a significant cost benefit. Locating the saddle coils in machined grooves in the monolithic shell provides precise positioning with minimum deflections. The main detraction of this option is the rather high current density in the saddle coils, which limits the peak field and pulse length. Access is marginally satisfactory, being limited mainly by the PBX TF coils and support structures, rather than the saddle coils. The PBX TF

coils limit the plasma to a narrow range in aspect ratio. New TF coils would relax the aspect ratio constraint and improve access, but at increased cost.

Several alternatives to a 1/R background coil topology such as the PBX option have been explored. The one that was most effective in reducing the current density was the L=3 option shown in Fig. 5. This option features 3 circular L=3 coils, 3 circular (vertical) TF coils, and 1 pair of circular PF coils for equilibrium control. The L=3 coils are tilted, interlocking coils that enclose the major axis and the plasma. Although the coils are planar and circular, they form a true helical winding around the plasma, closing on themselves after one poloidal and one toroidal circuit about the plasma. Conformal coils are located in a monolithic shell as in the PBX option. The L=3 coils are very effective in reducing the maximum current density in the saddle coils when compared with the $1/R$ backbgound TF option. Reductions of greater than 60% have been achieved. There are two detractions to this option. First, the presence of saddle coils near the outboard midplane restricts access for neutral beam injection. Second, with so few background coils, there is a large stray field in the vicinity of the neutral beams. Future explorations of this topology would need to address these issues.

Modular coils were also considered (see Sec. 6 for a design method for modular coils based on optimization). A full set of PF coils would be added for flexibility and inductive current drive. A supplementary TF set might also be required for experimental flexibility. Modular coils have been used on W7-AS and HSX and are planned for W7-X. Low stray fields obviate concerns about neutral beam compatibility. Reductions in current density of about 50% have been achieved relative to the $1/R$ background TF option, perhaps avoiding the need to pre-cool below ambient temperature. Modular coils are typically located further away from the plasma (except inboard), providing more space for plasma shape flexibility. The modular coils required to reproduce NCSX plasmas are different than existing modular coils, having a larger toroidal excursion and sharper radii of curvature. The main detraction of the modular coils lies in the large number of unresolved technical issues related to coil fabrication (minimum radius of curvature and twist), assembly, support, and alignment. Access for heating and diagnostics is also a concern.

6 COILOPT: A code for Designing Modular Coils

The coil design techniques discussed in previous sections have focussed largely on the use of saddle coils with a background toroidal field. Modular coils provide both poloidal and toroidal magnetic field components and pose additional design issues. Unlike saddle coils, no acceptable modular coil designs based on conformal winding surfaces have been found for compact stellarator configurations: magnetic field errors for a reasonable number of coils are simply too large. This results from a tradeoff between current density, which requires a relatively close plasma-coil spacing, and ripple errors that favor large plasma-coil separations.

To address these issues, COILOPT, a coil optimization code was developed[9]. The primary difference between this and similar codes such as ONSET[10] is in the representation of the coils. Coils lie on a winding surface with (typically) the toroidal location being given as a Fourier series in the poloidal angle. The winding surface is described by the usual Fourier series in the poloidal and toroidal angles for R and Z, namely,

$$R = \sum R_{mn} \cos 2\pi(mu + nv), Z = \sum Z_{mn} \sin 2\pi(mu + nv). \quad (4)$$

The toroidal position of a coil on this surface, the winding law, is given by

$$v(u) = v_0 + \sum_k [a_k \cos(2\pi k u) + b_k sin(2\pi k u)]. \quad (5)$$

This representation leads to a coil set that depends on, typically, of order a hundred independent parameters for the winding surface and the coil winding law. This is a factor 10-100 less than the number of parameters that are required to describe a coil set composed of a set of short segments. As a result of this reduction in the number of independent parameters, coil designs can be produced using a few hours of IBM RISC 6000 time.

The optimization uses the Levenberg-Marquardt algorithm[3]. In addition to targeting the magnetic field error B_{err}^{rms}, measures of plasma coil separation and coil to coil separation are used to control current density. Similarly, measures of coil curvature and length are used to control the variation of the winding surface and to produce coils acceptable from an engineering standpoint. Allowing the winding surface shape to vary during the optimization is key to the successful application of COILOPT. A modular coil set developed by COILOPT for the LI383 configuration is illustrated in Fig. 6. The current density in the copper is about $12kA/cm^2$, in the range that would permit coils to operate at room temperature.

7 Integrated Coil-Plasma Design Methods

The traditional methodology for coil-plasma system design is based on a two-stage approach. In the first stage, a plasma configuration is identified by the fixed-boundary plasma optimizer. This provides a target boundary surface and normal distribution of $\vec{B}$ on the plasma surface derived from currents flowing in the plasma volume. In the second stage coils are sought which attempt to match normal magnetic fields on the specified plasma boundary. Once the coil geometry is determined engineering figures of merit are analyzed, such as current density, minimum radius of curvature, etc. If these are unsatisfactory, the configuration is modified and the process is repeated. Iteration usually leads to a solution that meets a set of engineering requirements.

In NCSX design we have had success incorporating some engineering constraints into the fixed-boundary plasma optimizer, a procedure which greatly improves the efficiency of the two-stage coil design process. For example, a call to NESCOIL at each major step of the physics optimizer provides input to an auxiliary penalty function which measures the magnitude of J^{max}, the maximum current sheet density, and $\mathcal{C}$, the current sheet "complexity"[11] (mathematically the enstrophy of the current potential, a measure of the lumpiness of the current potential).

Additional penalty function strategies are being developed[12] which relate to issues of plasma control. The basic idea is to penalize configurations developed by the optimizer which require short wavelength magnetic fields for their reconstruction. At some level, it is clear that such fields at the plasma surface cannot be relevant to global physics properties of the plasma. If arbitrary independent plasma deformations are allowed by the fixed-boundary plasma optimizer, one cannot guarantee that the plasma shape output by the optimizer will avoid a dependency on these short wavelength fields. If these fields are required by the specific target shape and a coil set is designed to include provision of these fields, detailed control of the plasma shape can become problematic: Changes in short-wavelength fields at the plasma surface require substantial changes in current in

distant coils because of the rapid attenuation of such fields. Thus, it is worthwhile to consider the addition of a penalty function to the plasma optimizer which eliminates the possibility of designing to a configuration that requires small wavelength fields.

Given a CWS upon which a current sheet distribution is to be calculated, a physics-based complete set of functions, called "natural functions"[12] can be identified with the following properties: (1) They are eigenfunctions of an in-surface Helmholtz operator whose elements depend only on the winding surface geometry. A surface current distribution can be expanded in this complete set of functions. (2) Each function is labelled by an associated eigenvalue which tells us how rapidly the magnetic field strength due to that distribution of current decreases with distance from the surface. (3) The lowest order natural functions have the smallest eigenvalues and decay most slowly with distance from the surface. Figure 7 shows a contour plot of a low-order natural function, including a comparison with a related NESCOIL sine basis function.

We are presently exploring various methods for constraining configuration shapes such that their associated current sheet solutions can be fit exactly with only low-order (i.e., small eigenvalue) natural functions, say the lowest $N_f \sim 50$ or so. This can be done within the context of a free- or fixed-boundary optimization code. For example, once a CWS is defined the natural function current distributions can be calculated and a free-boundary optimizer can vary the N_f coefficients of the natural functions to minimize physics penalty functions (measuring quasisymmetry, stability and other physics or engineering measures such as current sheet complexity). Alternatively, in a fixed-boundary optimizer, for each step that the plasma configuration changes shape a CWS can be generated, and the assocoated natural functions calculated. A penalty function can then be evaluated representing the failure to fit the calculated B-normal at the plasma boundary with the lowest N_f of these functions.

8 Acknowledgements

We would particularly like to thank Peter Merkel and Michael Drevlak for use of NESCOIL and ONSET and for their support of our design efforts. This work was supported by US Department of Energy Contracts Nos. DE-AC020-76-CHO3073, DE-FG02-95ER54333, DE-FG03-95ER54296 and DE-AC05-00OR22725.

References

[1] NUHRENBERG, J.,ZILLE, R., Phys. Lett. A **129** (1988) 113-117.

[2] MERKEL, P., Nucl. Fusion **27** (1987) 867-871.

[3] PRESS, W.H., et al., "Numerical Recipes" (Cambridge University Press, 1996), p.51ff

[4] VALANJU, P., et al., "Stellarator Coil Design using Enhanced Green's Function Techniques" (in preparation).

[5] NEILSON, G.H., et al., "Physics issues in the design of high-beta, low-aspect-ratio stellarator experiments" Phys. Plasmas **7** (2000) 1911-1918.

[6] MYNICK, H., POMPHREY, N., "Control Matrix Approach to Stellarator Design and Control" (to appear in Phys. Plasmas).

[7] GOLDBERG, D.E., "Genetic Algorithms in Search, Optimization, and Machine Learning", (Addison Wesley, New York, 1989).

[8] MINER, W.H., et al., "Use of a Genetic Algorithm for Compact Stellarator Coil Design" (submitted to Nuclear Fusion, Oct 2000)

[9] STRICKLER, D.J., BERRY L.A., HIRSHMAN, S.P., "Optimization of Modular Coils for Compact Stellarators" (in preparation)

[10] DREVLAK, M., Fusion Technology **33** (1998) 106-117.

[11] HIRSHMAN, S.P., Private Communication

[12] BOOZER, A.H., "Stellarator Coil Optimization by Targeting the Plasma Configuration", Phys. Plasmas **7** (2000) 3378-3387.

Figure Captions

Figure 1: SVD scan for LI383 current sheet solutions with saddle topology showing trade-off between B-fitting error (B_{err}) and maximum current density (J_{max}) as the singular value cutoff is increased.

Figure 2: Poloidal cross-sections at toroidal symmetry planes of a c82 plasma boundary (solid curve), and boundary perturbed by $0.002\xi^{\mathbf{QA},\mathbf{K}}$ and $0.01\mathbf{v}^{\mathbf{QA},\mathbf{K}}$. The perturbation amplitudes used here were chosen for viewing purposes only.

Figure 3: Contours of current potential obtained by the SVD method of Sec. 2 form the coil pool for the GA. The particular coils selected by the GA for $N_c = 4$ are shown as thick lines.

Figure 4: Option with saddle coils and a $1/R$ background TF field. Circular PF coils are included for equilibrium flexibility.

Figure 5: L=3 background coil option with saddle coils. The coils shown include 3 circular, tilted, interlocking background coils; 3 circular (vertical) TF coils, 1 pair of circular PF coils, and the conformal saddle coils.

Figure 6: Modular coils calculated by COILOPT for LI383. There are seven coils/period and four unique coils.

Figure 7: In the upper frame, contours of a low-order natural function for the LI383 winding surface are shown. In the limit of infinite aspect ratio, this function corresponds to the $m = 1, n = 1$ NESCOIL sine function shown in the bottom frame,

Table Caption

Table 1: Comparison of mean and max fitting errors at plasma boundary, and max coil current density for various numbers of coils per half-period.

Method	N_c	$B_{err}^{rms}\%$	$B_{err}^{max}\%$	$I_c^{max}[kA/cm^2]$
Equi-Φ	13	0.95	7.0	14.7
GA	7	0.52	2.8	14.2
GA	6	0.61	3.8	12.7
GA	5	0.77	5.7	13.2
GA	4	0.92	5.0	14.2

Table 1

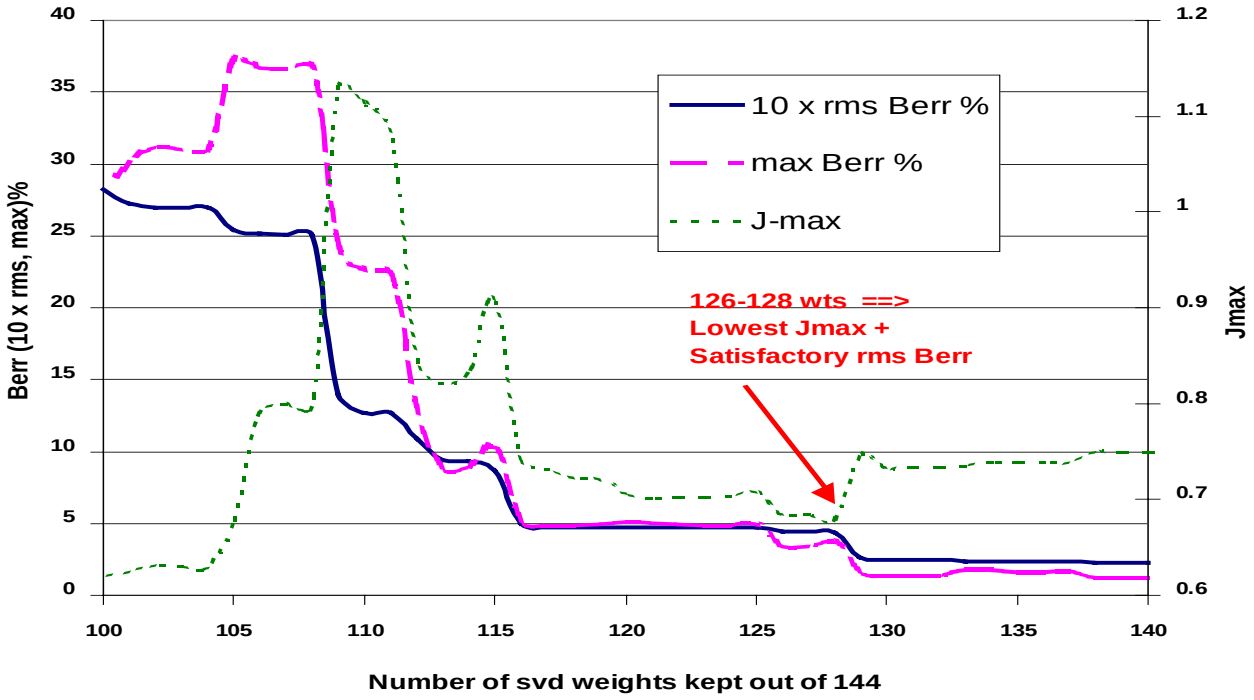
40
35
30
25
20
15
10
5
0
1.2
1.1
1
0.9
0.8
0.7
0.6
Berr (10 x rms, max)%
Jmax
100
105
110
115
120
125
130
135
140
Number of svd weights kept out of 144
10 x rms Berr %
max Berr %
J-max
126-128 wts ==>
Lowest Jmax +
Satisfactory rms Berr

Figure 1

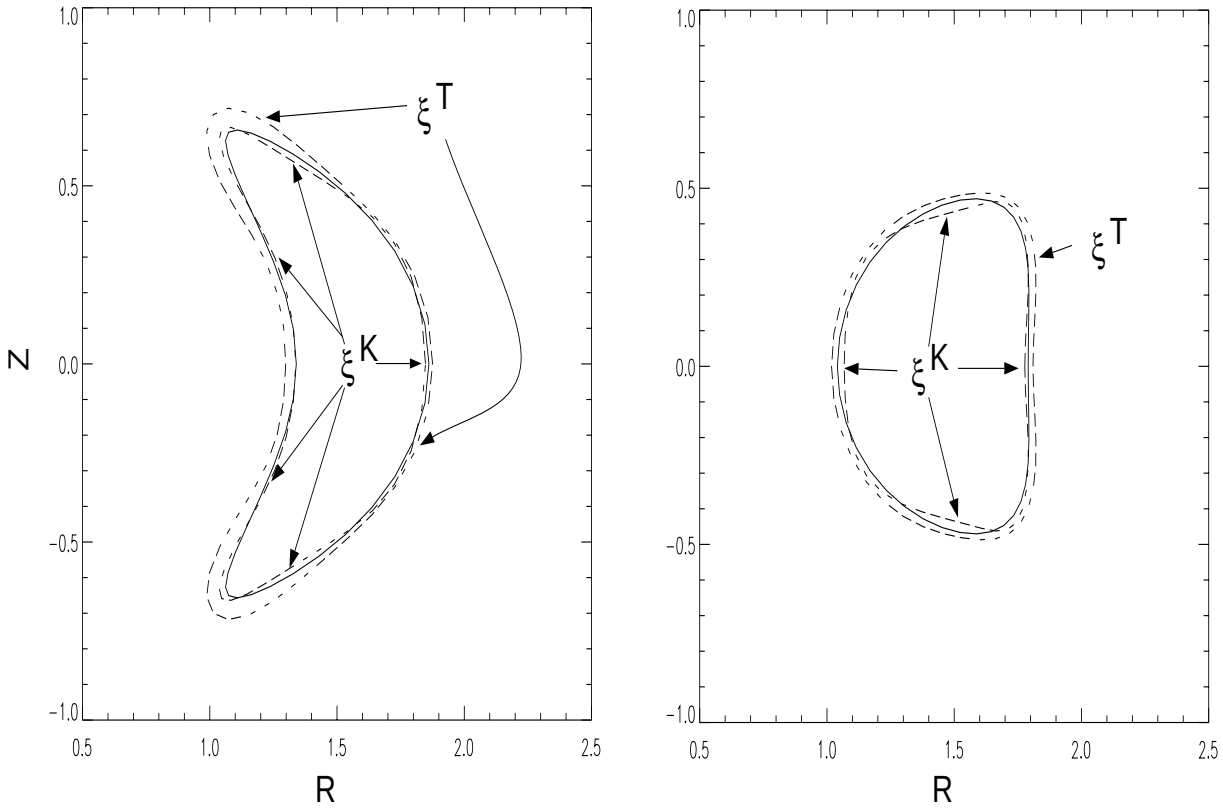

Figure 2

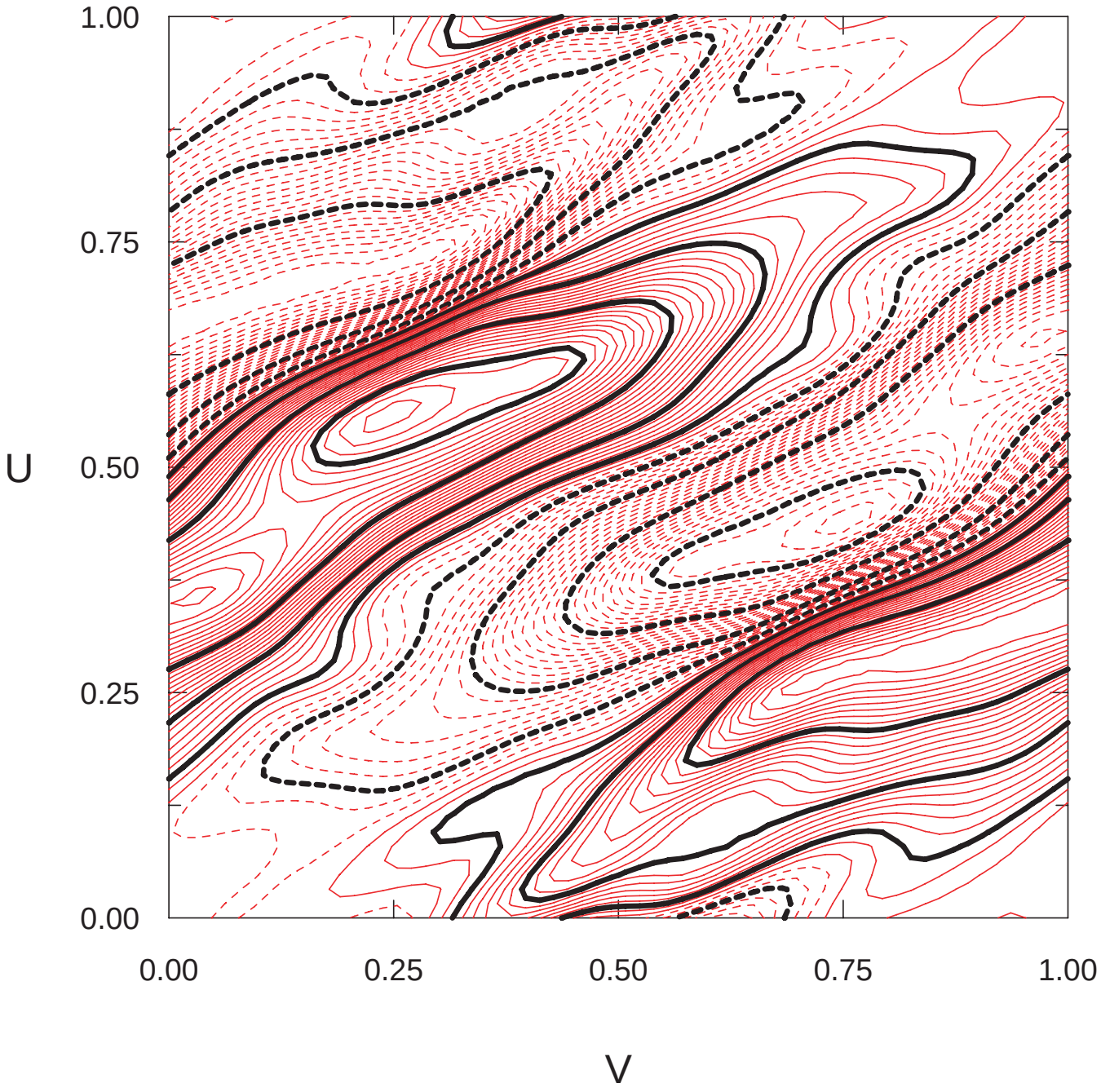

Figure 3

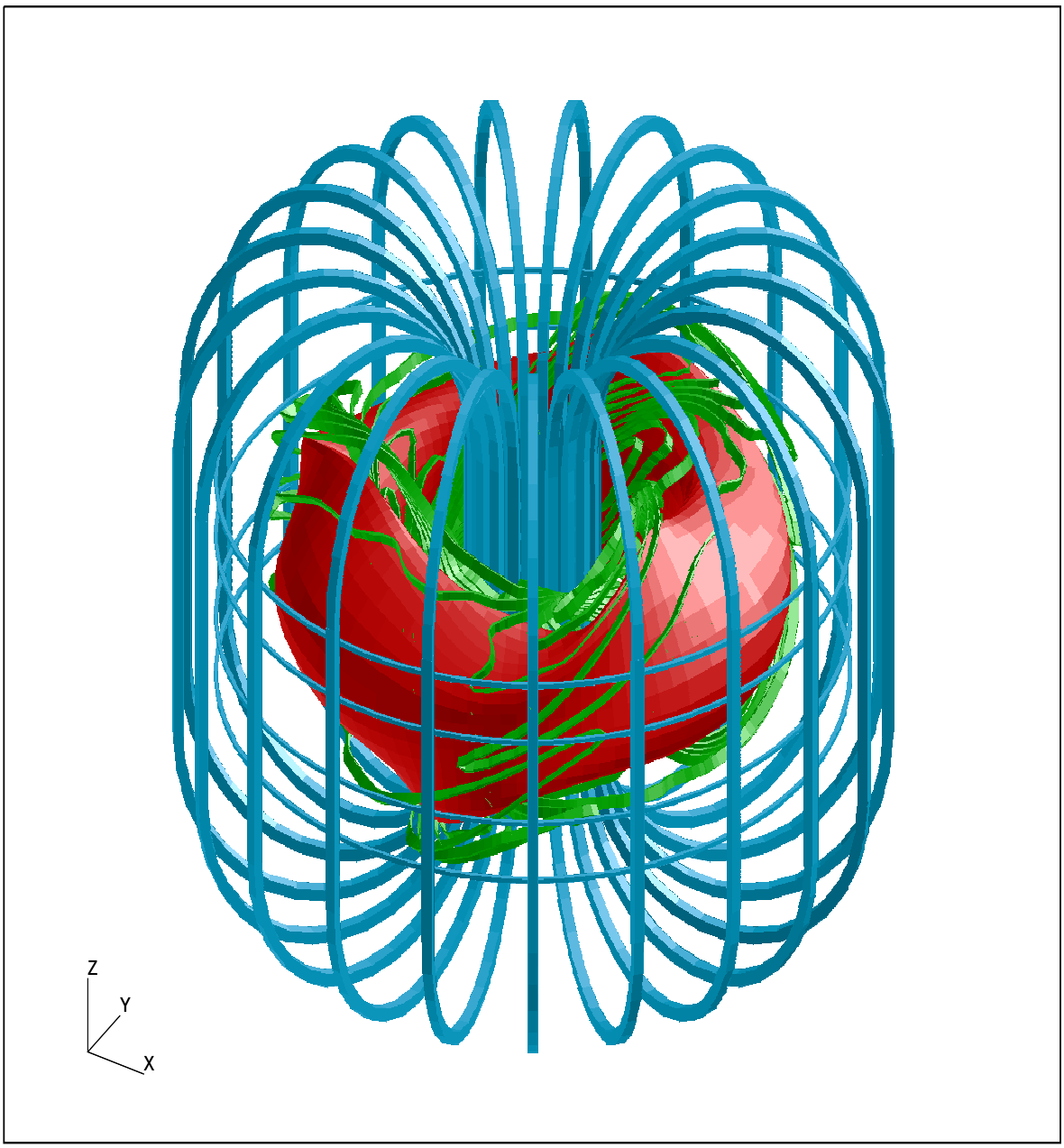

Figure 4

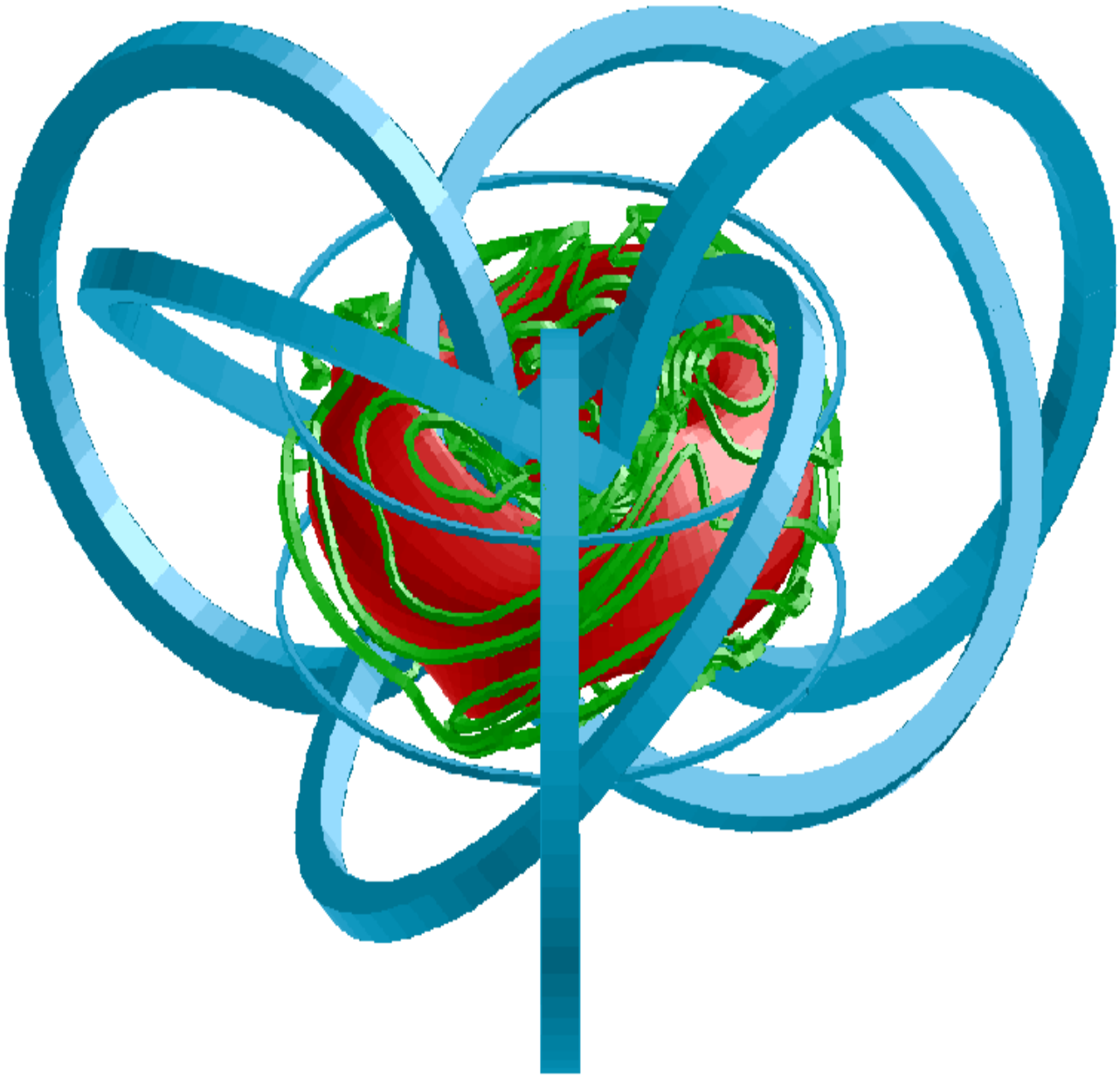

Figure 5

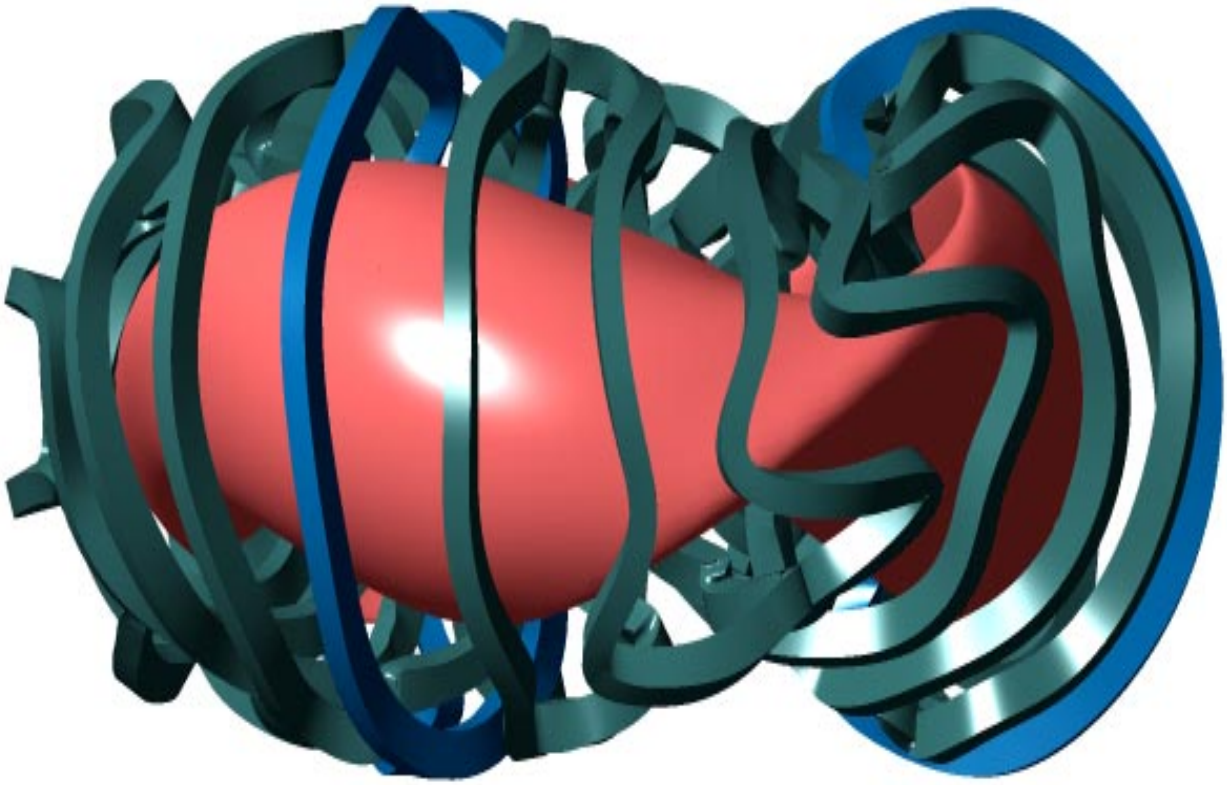

Figure 6

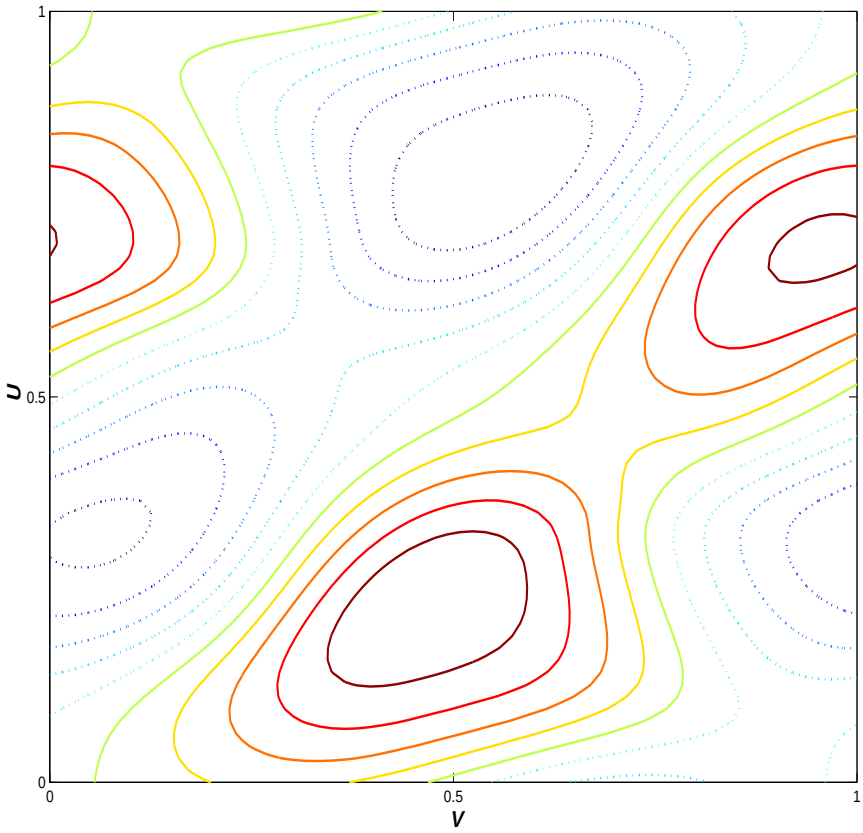

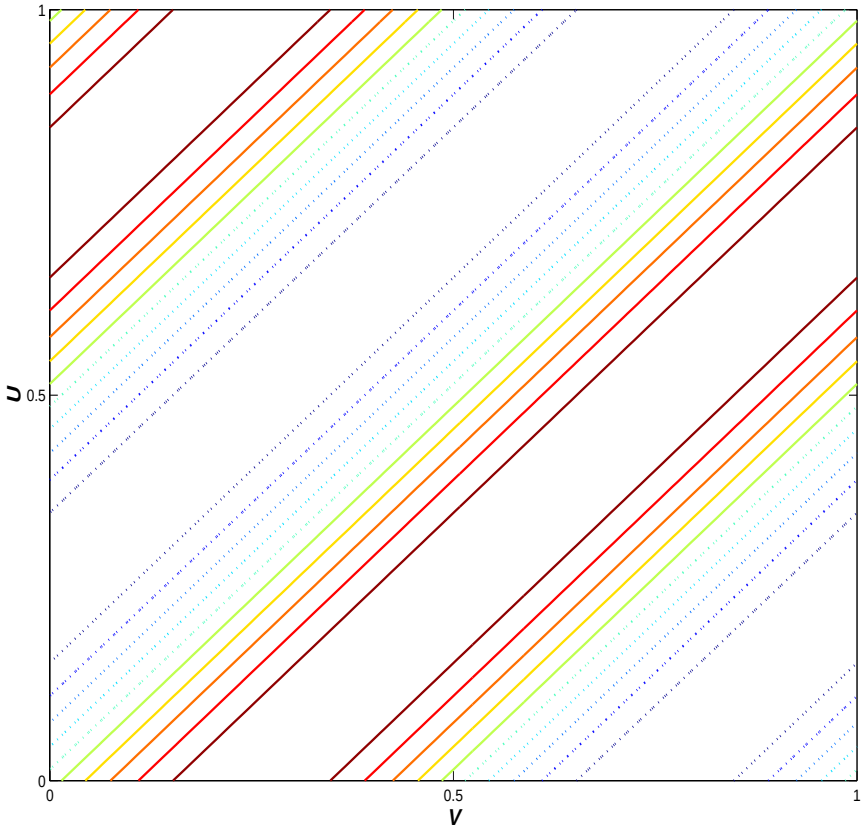

Figure 7